Friction Stir Welding of Very Thin Plates

(Ligação de chapas finas por *Friction Stir Welding)*

Ivan Galvão[1], Carlos Leitão[1], Altino Loureiro[1], Dulce Rodrigues[1,]*
*[1] CEMUC, Dpt. of Mechanical Engineering, University of Coimbra – Portugal, * dulce.rodrigues@dem.uc.pt*

Resumo

Os resultados obtidos no presente estudo, referentes a friction stir welding de chapas de alumínio, cobre, cobre-zinco e zinco com 1 mm de espessura, provam que a aplicação desta tecnologia para a ligação de chapas muito finas é possível e desejável. De fato, independentemente do material de base, as soldas produzidas apresentaram características morfológicas muito boas e um significativo refinamento do grão na zona do nugget. Ensaios de dureza e tração provaram que todas as soldas apresentavam, no mínimo, propriedades mecânicas semelhantes às dos materiais de base. Com base nos resultados da liga de alumínio AA 5182 foi também possível concluir que ao aumentar a velocidade de soldagem, o que melhora a produtividade do processo, aumenta-se o refinamento do grão no nugget, melhorando as propriedades mecânicas das soldas.

Palavras-chave: *FSW; Chapas finas; Alumínio; Latão; Zinco.*

Abstract: *The results obtained in present research, relative to friction stir welding of 1 mm thick plates of aluminium, copper, copper-zinc and zinc alloys, prove that the application of the process in the joining of very thin plates is feasible and desirable. In fact, independently of the base material, the welds produced presented very good morphological characteristics and significant grain refinement in the nugget. Tensile and hardness tests proved that all the welds were at least in even-match relative to the base material properties. Based on the AA 5182 aluminium alloy results it was also possible to conclude that augmenting the welding speed, which improves process productivity, increases grain refinement in the nugget, improving the mechanical properties of the welds.*

Keywords: *FSW; Thin sheets; Aluminium; Copper; Brass; Zinc.*

1. Introduction

At the beginning of the 90´s the Welding Institute patented the Friction Stir Welding (FSW), a new and revolutionary joining process, whose development has been driven by its potential for joining materials considered hardly weldable by conventional fusion processes, in similar and dissimilar arrangements [1-4]. In this process, the welds are produced by plunging a non-consumable rotating tool, composed by a specially shaped pin and shoulder, into the abutting edges of the sheets to be joined and translating it all along the joint (Figure 1). The heating and mixing of materials are the main functions of the tool, more precisely, due to the combined effect of tool rotation and translation, localised frictional heating softens the material around the tool moving it from the front of the tool, to its trailing edge, where it is forged into a weld. Since the weld is formed by plastic deformation of the base materials at temperatures below its melting temperature, FSW is classified as a "solid-state" joining technology [2, 5-10].

According to Figure 1, the half part of the joint where tool rotation and translation have the same direction is designated as Advancing Side (AS), whereas the other side is denominated as Retreating Side (RS). As a result of the process mechanics and heat generation it was found that the friction stir welds are composed of two main zones which are usually designated as thermo-mechanically affected zone (TMAZ) and heat-affected zone (HAZ). Meanwhile in the HAZ the material experienced thermal conditions that modified its microstructure and/or the mechanical properties without any plastic deformation, in the TMAZ, the material was plastically deformed at high temperatures under the action of the welding tool. Usually, in TMAZ it is possible to distinguish a boundary between two sub-regions, one characterized by the presence of elongated grains, deformed in the tool rotation direction, and one other with a fully recrystallized microstructure. The fully recrystallized region, usually named Nugget or Stirred Zone, is frequently considered a separate FSW microstructural zone [7, 11].

The minimal distortion of the welded components, which is related to the existence of low heat input during welding, and the high reproducibility of the weld characteristics make FSW both technically and economically very attractive for some industrial sectors. In particular, over the last 20 years, FSW of aluminium and its alloys has captured important attention from manufacturing industries, such as shipbuilding, automotive, railway and aircraft production [2, 5, 12-14]. Supporting its

(Recebido em 06/08/2011; Texto final em 02/03/2012).

industrial application, several studies have been conducted in friction stir welding of aluminium, being already concluded that the mechanical properties of the friction stir welds in heat-treatable aluminium alloys depend mainly on the size, volume fraction and distribution of precipitates in the stirred region and adjacent heat affected zone [15-19]. Research developed in friction stir welding of non-heat-treatable aluminium alloys enabled to determine that the mechanical properties of the welds produced depend mainly on the grain size and on the density of dislocations after the plastic deformation and recrystallization processes taking place during welding [10, 18, 20].

Although, as referred above, the industrial application of FSW is mainly focused in the joining of aluminium alloys, in recent years, the process research area has also been extended to the welding of other materials, such as copper and copper-zinc (brass) alloys in similar and dissimilar configurations [21, 22]. Specifically, in copper FSW literature, the relation between the mechanical properties and the grain structure of the welds is particularly enhanced by several authors. Example of this were Lee and Jung [21] that, studying the joining of 4 mm thick pure copper plates, observed the formation of a slightly softened region in the stirred zone, in spite of the smaller grain size compared to that of the base metal. They have also reported that the hardness of the stirred zone mainly depends on the density of dislocations rather than on the grain size. Nevertheless, more recently, Xie, Ma and Geng [23] mentioned that the grain refinement in the nugget of FS welds in 5 mm thick plates of pure copper resulted in increased hardness and yield strength relative to the base material.

Park et al [24] studied the microstructure and mechanical properties of friction stir welds in 2 mm thick CuZn40 alloy plates. These authors observed overmatched mechanical properties in the stirred zone of the welds relative to the base material. Furthermore, they claimed that increasing the rotational to welding speed ratio led to a strong decrease in the stirred zone grain size, which resulted in better strength properties. Meran [25], who studied FS welds in 3 mm thick plates of CuZn30, also pointed a strong influence of the pin screw geometry on material flow during welding, and so in the weld characteristics. More recently, Çam, Mistikoglu and Pakdil [26], that studied FS welds in two different copper-zinc alloys, the CuZn10 and CuZn30 alloys, both 3 mm thick, attributed an important role to the zinc content of the base material in the weldability of this type of alloys.

The literature cited in previous paragraphs points the important advances that have been achieved in FSW of thick plates. However, the application of the process for joining very thin sheets (1 mm thick or less) is still very scarcely explored, despite the joining of very thin plates, in similar and dissimilar configurations, has great interest in the production of tailor welded blanks (TWBs) that can be transformed, using plastic deformation processes, in products with technical and/or design interest. Nevertheless, to allow this kind of processing, the welds produced must have good surface finishing, as well as good plastic behaviour, which means low incidence of defects and improved mechanical properties [27-29]. The lack of work in very thin plates joining is probably a consequence of the major difficulty in optimizing welding parameters, such as tool geometry, tool dimensions and positioning or/and axial load for this type of plates. In fact, in this case, the amount of material moved by the tool is so small that controlling the material flow and obtaining non-defective welds is harder than in thick plates joining. Another aspect usually referred as a limitation in friction stir butt welding of thin sheets is the thickness reduction in the weld, resulting from the forging effect of the shoulder, which can significantly reduce the mechanical resistance of plates 1 mm thick or less, especially for under-matched welds.

The aim of present research was to prove the feasibility of friction stir welding very thin sheets of aluminium, copper and copper-zinc alloys. The effect of the welding speed on the microstructure and mechanical properties of FS welds in 5182-H111 aluminium alloy was also studied. Preliminary FSW tests were also performed in a zinc alloy.

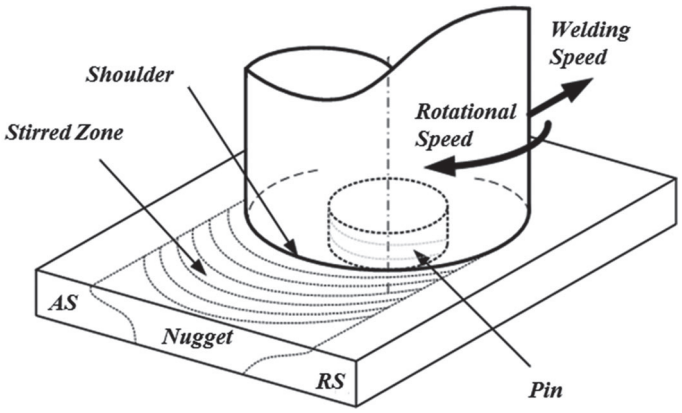

Figure 1 - FSW process scheme.

2. Experimental Procedure

In this study, friction stir welds were performed in 1 mm thick plates of heat-treatable (6016-T4) and non-heat treatable (5182-H111) aluminium alloys, phosphorus deoxidised copper (Cu-DHP, C12200), brass (CuZn37) and zinc (Zintek). The welds were performed in butt joint arrangement, using a conventional vertical milling machine. Optimized tool geometries and welding parameters were chosen based on previous experience of the workgroup. Due to the huge importance of tool traverse speed in process productivity, a special set of welds was performed by using increasing tool traverse speeds. The base material used in this study was the 5182-H111 aluminium alloy, which is a very popular alloy for automotive applications. Conical tools were used in most of the welding operations (Figure 2.a), except for the varying traverse speed tests, for which a scrolled tool was used (Figures 2.b and c). The welding parameters used in the tests are shown in Table 1. As shown in the table, each weld will be identified based on the base material (AXX for aluminium, B for brass, C for copper and Z for zinc) and rotational (ω) and traverse speeds (v) used in its fabrication, i.e., the acronym A82-180-16 identifies the 5182-H111 welds performed using rotational and traverse speeds of 1800 rev.min^{-1} and 160 mm.min^{-1}, respectively.

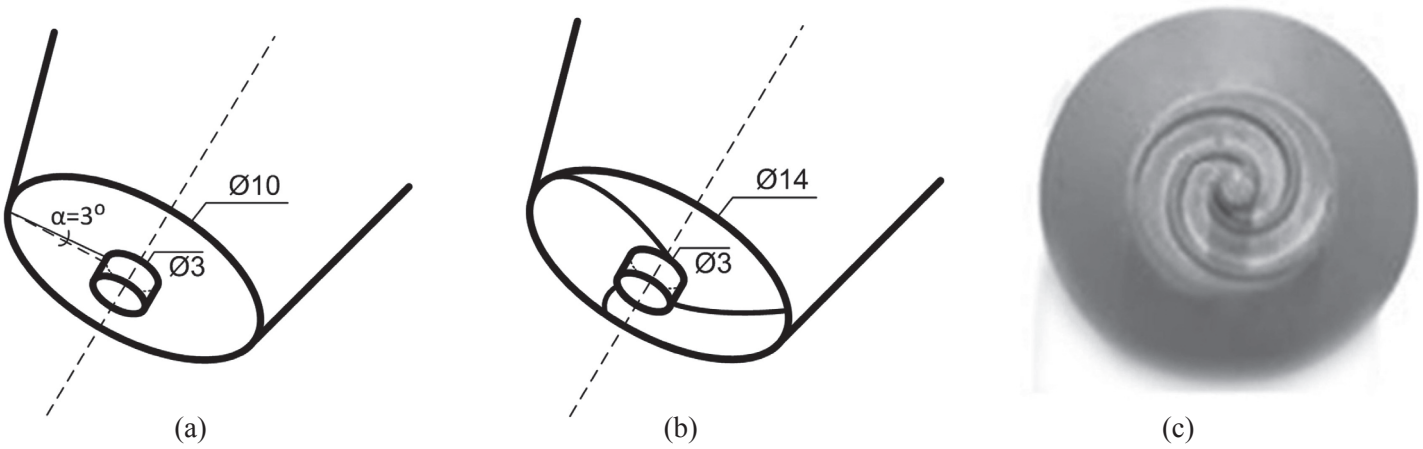

Figure 2 - Scheme of a C10 Conical tool (a) and scheme (b) and picture (c) of a S14 Scrolled tool.

Table 1 - Welding parameters.

Weld ID	Base Material	Tool	ω	v	Tool tilt angle
			rev.min^{-1}	mm.min^{-1}	
A82-180-16	5182-H111	C10	1800	160	2.5º
A16-180-16	6016-T4		1800	160	2.5º
C-100-25	Cu-DHP		1000	250	2º
B-114-30	CuZn37		1140	300	2º
Z-150-30	Zintek		1500	300	2º
A82-112-32	5182-H111	S14	1120	320	0º
				480	
				640	

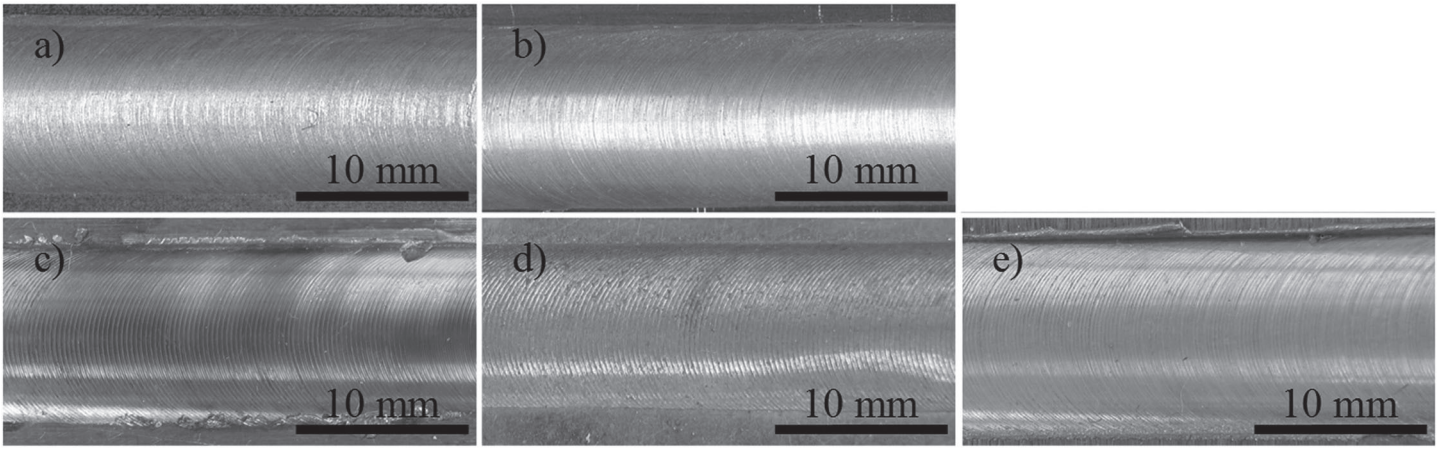

Figure 3 - AA 5182-H111 (a), AA 6016-T4 (b), copper (c), brass (d) and zinc (e) friction stir welds.

Visual inspection and root bending tests were performed in order to ensure that the welds were free of defects. Microstructural analysis was done by means of optical microscopy, using a ZEISS HD 100 equipment, and transmission electron microscopy, using a FEI-TECNAI G^2 apparatus. The specimens were prepared by standard metallographic techniques and etched with reagents specific to reveal the microstructure of each alloy. Vickers micro-hardness was measured, perpendicular to the welding direction, using a Shimadzu micro-hardness tester with 200gf. for 15 seconds. Tensile specimens of 50 mm gauge length were machined from the friction stir welded plates, normal to the welding direction. The tensile tests were carried out on a Shimadzu Autograph AG-X universal testing machine. One ARAMIS Optical 3D system was used for strain data acquisition.

3. Results and Discussion

3.1. Weld morphology and microstructure

Visual inspection revealed that, independently of the base material, all the welds displayed excellent appearance with very fine and regularly distributed arc shaped striations, as is

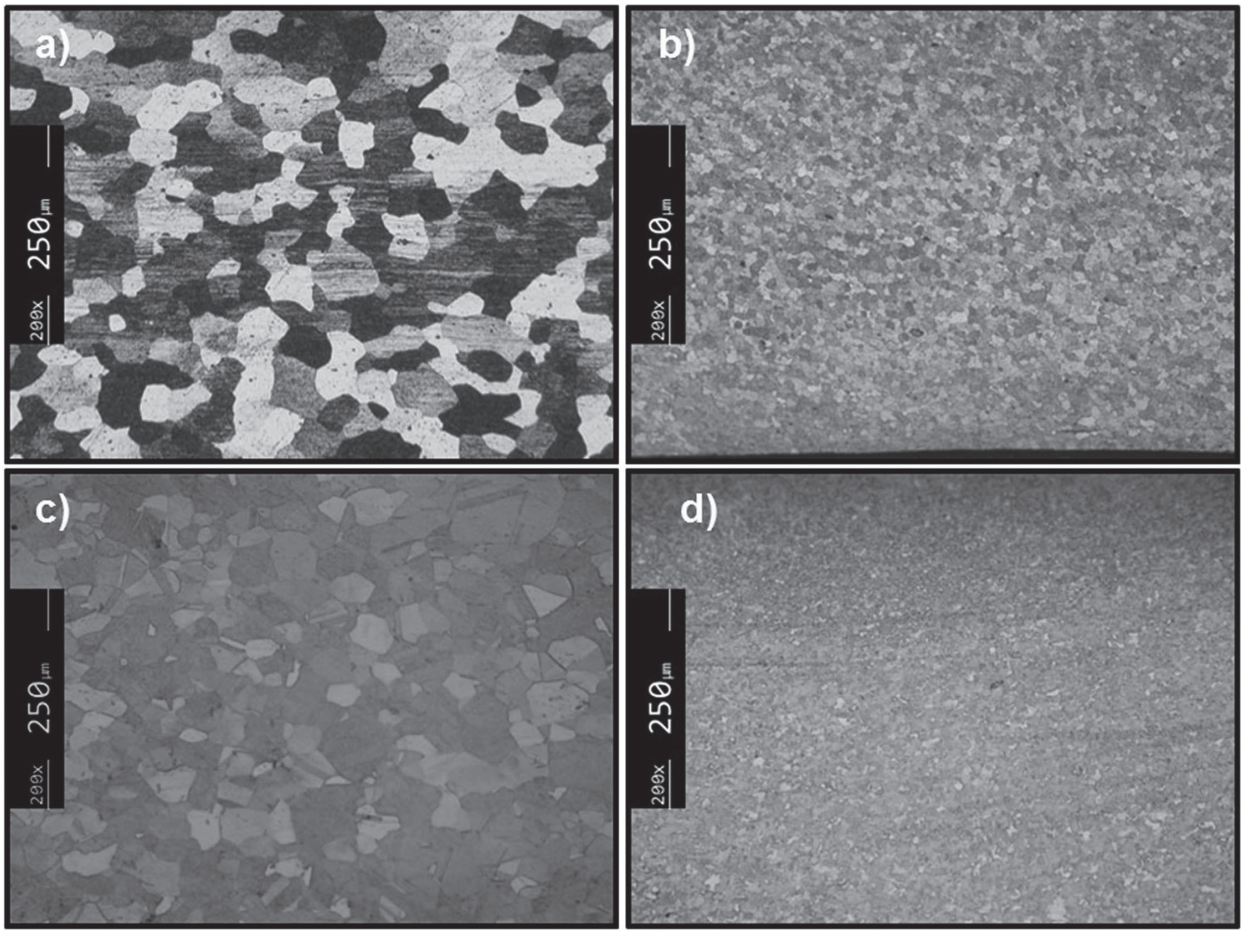

Figure 4 - Microstructures of the AA 5182-H111 (a) and brass (c) base materials and respective weld TMAZs (b and d).

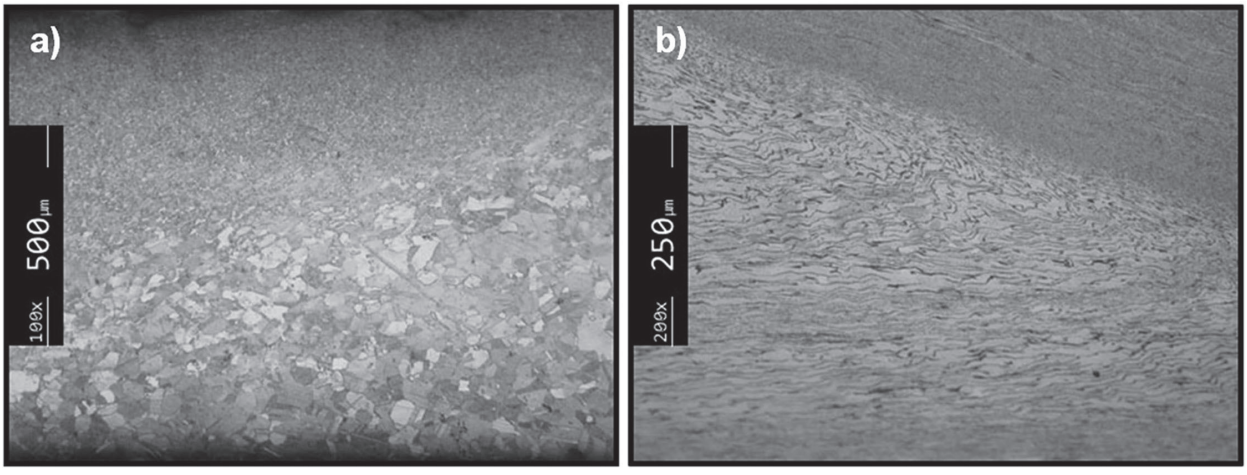

Figure 5 - Transition between the TMAZ and HAZ at the retreating side of a brass weld (a) and at the advancing side of a zinc weld (b).

illustrated in Figure 3. The welds in 6016-T4 aluminium alloy, copper and zinc also showed very small flash at the advancing side. Because of tool tilt angle, a small reduction in thickness, lower than 5%, was measured in all the welds produced with the conical tool. No cracks were detected in the root bending tests of the welds, except for the zinc welds, which displayed intermittent kissing bond, showing that tool penetration depth was insufficient.

Metallographic analysis revealed that the welding process yielded extremely fine grains in the centre of the stirred zone of all the welds. This grain refinement, which results from dynamic recrystallization occurring during welding, is exemplified in Figure 4, where the microstructure of the base materials and welds are shown for the 5182-H111 aluminium alloy (a and b, respectively) and brass (c and d, respectively). A substantial change of the base material microstructure was also observed

at the transition between the TMAZ and the HAZ, as is shown in Figures 5.a and b, for the brass and zinc welds, where it is possible to observe the severely deformed microstructure of the non-recrystallized grains of the TMAZ. Some grain coarsening was also observed in a narrow region of the HAZ of the brass welds, as is illustrated in Figure 5.a. The average grain sizes, for all base materials, except zinc, and respective thermo-mechanical affected zones are resumed in Table 2. In fact, the most significant grain refinement was observed in the TMAZ of the zinc welds, for which it was not possible to determine the grain size using optical microscopy.

Table 2 - Average grain sizes.

	5182-H111	6016-T4	Cu-DHP	CuZn37
Base Material	37 µm	23 µm	18 µm	24 µm
TMAZ	7 µm	7 µm	5 µm	7 µm

3.2. Hardness

The microstructural changes, which are function of the process parameters and base material nature, had distinct impacts in the mechanical properties of the different welds, as is show in Figure 6**,** where the hardness profiles across the welds are displayed. The vertical lines in the graphs represent the limits of the shoulder influence area and the horizontal lines illustrate the average hardness of each base material. As shown in the graph, for the brass welds, hardness values higher than those of the base material were registered in the TMAZ, which can be attributed to the very small grain size illustrated in Figure 4.d. For the same welds, hardness values smaller than that of the base material were registered in the HAZ, at the limit of the shoulder influence area, where a coarser grain structure was depicted (Figure 5.a). Park et al [24] also registered a hardness increase in the nugget of friction stir welds in 2 mm thick 60% Cu-40% Zn plates, but did not notice any softening in the HAZ. Since the welding speeds in that research were much higher than those used in present work, it is supposed that the heat input was smaller, which probably avoided the occurrence of grain coarsening in the HAZ.

Analysing now the hardness profile of the copper welds, also illustrated in Figure 6, it is possible to notice a significant hardness increase in the TMAZ, which can be attributed to the grain refinement in the nugget and strain-hardening of the plastically deformed zone outside the nugget depicted in the microstructural analysis. For these welds only a slight softening was registered in the HAZ. As in present work, Xie, Ma and Geng [23] also depicted grain refinement and hardness increase in the nugget of welds in thick plates of pure copper.

The hardness results for the 5182-H111 and 6016-T4 welds show that the FSW process induced very small changes in base material properties, since no important hardness variation was registered across both welds. Though the hardness distribution in the welds is similar for both alloys, the strengthening mechanisms for each alloy are quite different. For the 5182-H111 alloy, a non-heat treatable alloy, it is possible to assume that the hardening produced by the intense plastic deformation occurring during FSW was compensated by the annealing effect, which resulted from the recrystallization process, preventing hardness increase in the TMAZ. The mechanical properties of the welds in the 6016-T4 alloy, which is a precipitation-hardenable alloy, are more influenced by the volume fraction, size and distribution of strengthening precipitates, than by the grain refinement in the nugget. As no substantial change in hardness was observed in these welds, it is possible to assume that the heat generated was high enough to promote full solubilisation of the small precipitate clusters of the naturally aged alloy. New precipitation on cooling produced a microstructure in the weld similar to that of the base material, and so, similar hardness levels. For both alloys, the hardness profiles can be explained assuming high heat-input during the process, which can be associated with the high tool rotation and low tool traverse speeds used when performing the welds [30]. In fact, according to Rodrigues et al [15], the weld properties, for both the 5182-H111 and 6016-T4 alloys, can be drastically altered by changing the process parameters and tool geometry.

Finally, no significant changes in hardness were observed in present work for the welds in zinc. Since this material is a work hardenable metal, like the 5182-H111 alloy, it is possible to assume that the hardening effect produced by the plastic deformation of the base material was mitigated by annealing resulting from the heat generated during FSW.

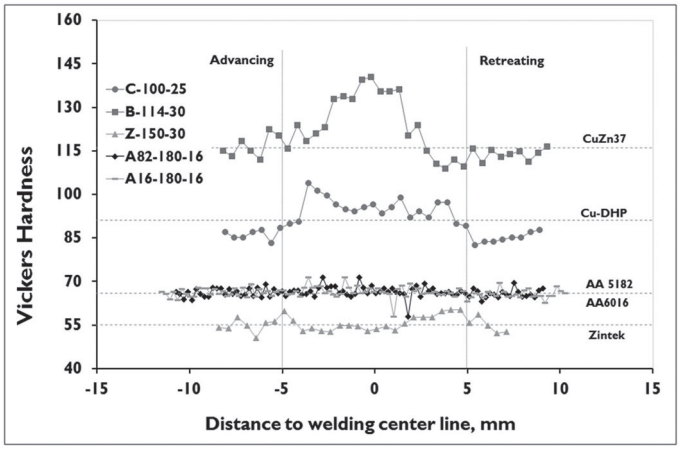

Figure 6 - Hardness profiles in the cross section of the welds.

3.3. Tensile test results

The engineering stress-strain curves from the tensile tests of transverse specimens removed from the different welded plates, are plotted in Figure 7. The yield stress (σ_Y), the tensile strength (σ_m) and the elongation at maximum load for the welded samples and base materials are compared in Table 3. In the table, the yield (η_Y) and strength (η_m) efficiencies, computed by dividing the yield and tensile strengths of each weld by those of the corresponding base materials, are also displayed. Figure 7 and Table 3 show that, though the elongation of the welded specimens was always inferior to that of the respective base materials, all the welds had good global ductility, except the zinc welds. Table 3 also demonstrates that all the welds, except

Table 3 - Tensile properties of the base materials and welds.

Welds	σ_Y (MPa)		σ_m (MPa)		Elong. (%)		η	
	BM	Weld	BM	Weld	BM	Weld	η_Y	η_m
A82-180-16	108	114	275	264	24	17	1.0	0.96
A16-180-16	106	108	225	208	24	13	1.0	0.92
C-100-25	196	200	244	256	30	20	1.0	1.05
B-114-30	236	240	375	368	43	20	1.0	0.98
Z-150-30	156	117	167	153	40	3	0.75	0.92

those in zinc, displayed even-match properties relative to the yield stress of the respective base materials and moderate under-match conditions relative to the tensile strength. The poor tensile performance of the zinc welds can be attributed to the kissing bond defect depicted in the bending tests.

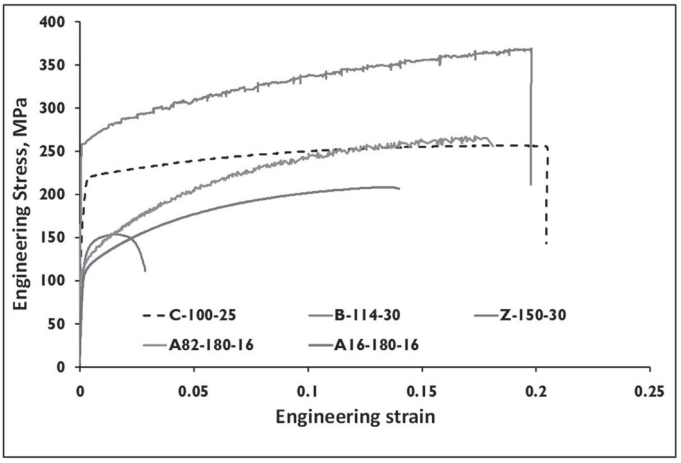

Figure 7 - Engineering stress-strain curves for specimens removed transverse the welding direction.

Tensile testing of the brass samples revealed that they failed in the base material, before the TMAZ had been plastically deformed. On the other hand, the welds in 6016-T4 alloy failed in the weld. Factors such as the thickness reduction in the welds or the kerfs effect of the striations on the top of the welds may have favoured the location of the fracture. These factors are much more important in the case of even-match welds in thin sheets, such as those on alloys 6016-T4 and 5182-H111. For the zinc samples, due to the kissing-bond defect, failure of the samples occurred for very small plastic deformation levels.

Figure 8 shows local tensile stress-strain curves corresponding to different areas of a transverse specimen, namely, the BM and TMAZ zones of a copper weld specimen, as well as an image of the longitudinal strain distribution in the specimen before maximum load, which was acquired using the optical extensometer. The hardness profile of the weld and the stress-strain curve corresponding to a homogeneous base material sample are also illustrated in the figure. The longitudinal strain distribution clearly shows lower values of strain in the TMAZ, where higher hardness values where registered relative to the base material.

Comparing the curves in the graph it is possible to conclude that the copper welds TMAZ was clearly in yield and tensile strength over-match relative to the base material and that the local curve corresponding to the BM is in perfect accordance with base material sample results. It is also important to enhance the existence of two different sub-regions (1 and 2) inside the TMAZ. In fact, at the advancing side of the TMAZ (1), higher values of yield and tensile strength and lower values of longitudinal strain were registered, relative to the retreating side of the TMAZ (2), which is in accordance with the higher values of hardness observed in that zone.

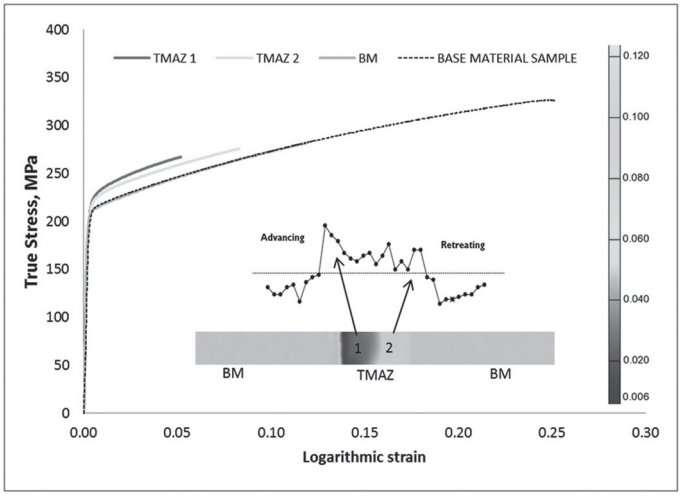

Figure 8 - Local stress-strain curves for a copper weld (a) and location of the measuring points and longitudinal strain distribution before maximum load (b).

3.4. Effect of traverse speed on weld strength

Results mentioned above prove the feasibility of FSW process for producing TWB in very thin sheets of various materials. However, it should be taken in mind that these results refer to selected sets of process parameters and that the microstructure and mechanical properties of the welds are influenced by both process parameters and base material initial condition. In industrial application, besides the mechanical properties of the welds, the productivity of the welding processes should be taken in consideration too. Because of this, the effect of the tool traverse speed on the microstructure and mechanical properties of welds in 5182-H111 aluminium alloy was studied. According

to Table 1, a scrolled shoulder tool was used and 320, 480 and 640 mm.min^{-1} traverse speeds were tested. The advantage of using a scrolled shoulder lies in this not induce any reduction in thickness in the welds. Figure 9 illustrates the hardness profiles across the welds. The dashed line in the figure represents the average hardness of the base material. The image shows a significant increase in hardness across all the welds, as opposed to the results represented in Figure 6 for the same alloy. The hardening effect is more important for the weld carried out with the highest traverse speed.

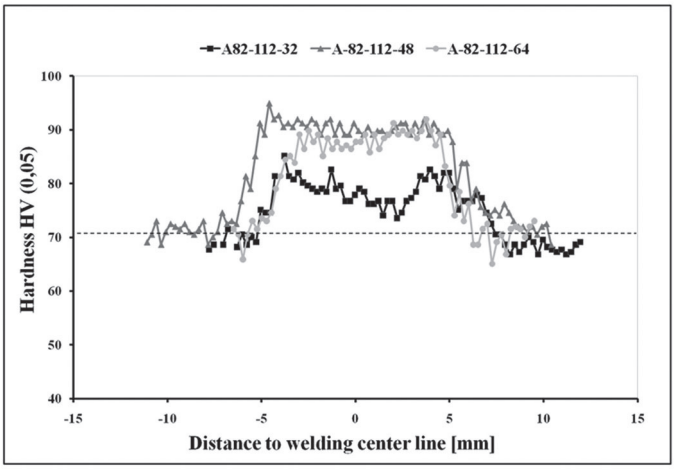

Figure 9 - Hardness profiles in the cross section of the welds.

Detailed metallographic analysis revealed that the TMAZ of these welds was composed by very fine and equiaxed grains, with average grain size of 5 µm and 3 µm for the lowest (320 mm.min^{-1}) and the highest (640 mm.min^{-1}) traverse speeds, respectively. Grain refinement results from the dynamic recrystallization process induced by both the extensive plastic deformation and the heat generated in the process, as mentioned by Murr et al [31]. TEM analysis revealed a sub grain structure inside the TMAZ, with high density of dislocations, as is exemplified in Figures 10.a and b, for the A82-112-32 and A82-112-64 welds. It was observed that increasing the traverse speed, the sub-grain size decreased increasing the welds hardness, as showed in Figure 9. The hardness profiles in Figure 9 also show hardness peaks close to the borders of the TMAZ, at the advancing and retreating sides of all the welds, where there are narrow bands of highly deformed non-recrystallized grains. Finally, the welds done with traverse speeds of 480 and 640 mm.min^{-1} exhibit approximately the same hardness, indicating that for each rotational speed there is a maximum traverse speed above which no additional increase in hardness is produced.

Table 4 shows the average tensile properties of the welds (TMAZ) and the corresponding mis-match in yield (M_{ys}) and tensile (M_m) strengths relative to the base material. According to these results, the welds were all in a strong yield strength over-match condition, which increases with increasing weld traverse speed, but in even-match conditions relative to the tensile strength. Those results are consistent with the evolution of hardness and the microstructural changes in the TMAZ. Despite the tensile strength even-match condition, the yield strength over-match of the welds lead to the fracture in the base material of the transverse specimens, since the BM experienced most of the plastic deformation during tensile testing. It is also important to enhance that, in a previous study, the formability of the 5182-H111 and 6016-T4 tailored blanks was assessed by deep-drawing axisymmetric cups. For a punch displacement of 60 mm, no necking was observed in the weld zone, as is demonstrated by Rodrigues et al [15] and Leal et al [29] where results and experimental details are described.

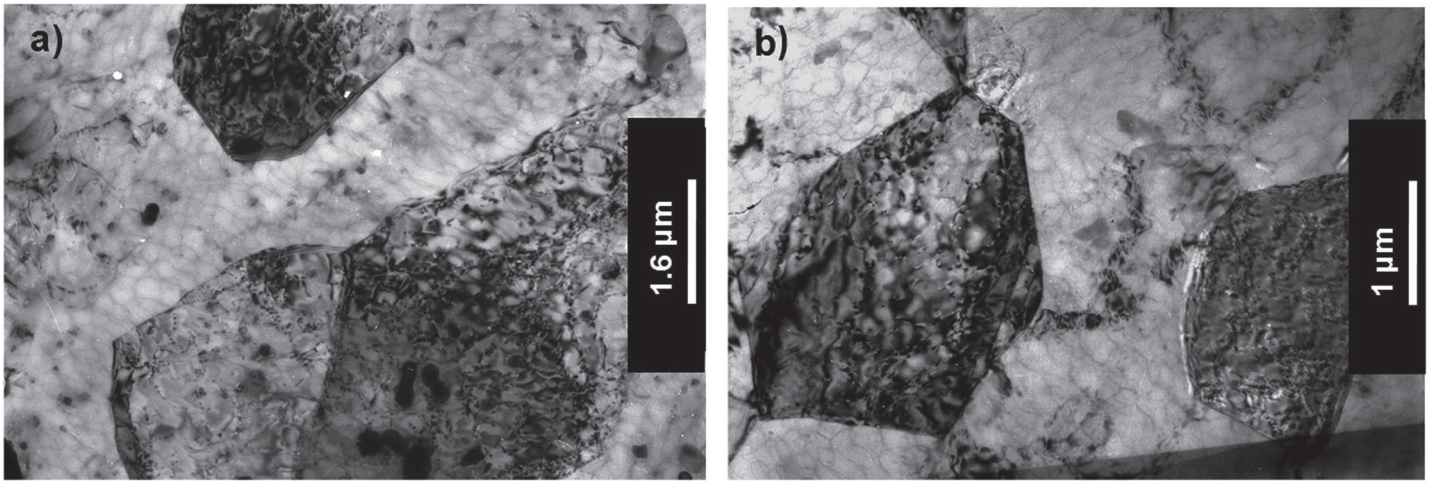

Figure 10 - TEM images from the TMAZ of the A82-112-32 (a) and A82-112-64 (b) welds.

Table 4 - Tensile test results of longitudinal weld specimens and mis-match levels.

Weld reference	σ_Y (MPa)	σ_m (MPa)	Elong (%)	M_{ys}	M_m
A82-112-32	161	267	18.7	1.49	0.97
A82-112-48	168	273	20.6	1.55	0.99
A82-112-64	192	286	18.7	1.83	1.04

4. Conclusions

The following conclusions can be drawn from present investigation:

1) Except for the welds in zinc, which had a small root defect, all the welds were free of defects;
2) The welds free of defects were at least in even-match condition relative to the base material;
3) FSW produced a significant grain refinement in the nugget of all the welds;
4) The grain refinement was associated with a hardness increase only for the welds in copper and brass, in the range of parameters tested;
5) The increase of welding speed raised the grain refinement in the nugget, and increased hardness and tensile strength, in 5182-H111 welds.

Results mentioned above prove the feasibility of FSW of very thin sheets in aluminium and copper alloys.

5. Acknowledgements

The authors are indebted to the Portuguese Foundation for the Science and Technology (FCT) through COMPETE program from QREN, to FEDER, for the financial support, and Thyssen Portugal – Aços e Serviços, Lda. company, for providing materials and heat treatments for the tools designed and fabricated in the project.

6. References

[1] THOMAS, W.M. Friction stir welding and related friction process characteristics. **In:** INALCO '98, 7th INTERNATIONAL CONFERENCE ON JOINTS IN ALUMINIUM, 1998, Abington - Cambridge. Proceedings. Available in: http://www.twi.co.uk/content/spwmtapr98.html. Accessed in: September 25 2010.

[2] KALLEE, S.W.; NICHOLAS, E.D.; BURLING, P.M. Application of friction stir welding for the manufacture of aluminium ferries. **In:** 4th INTERNATIONAL FORUM ON ALUMINIUM SHIPS, 2000, New Orleans. Proceedings. Available in: http://www. twi.co.uk/content/spswkmay2000.html. Accessed in: September 25 2010.

[3] THOMAS, W.M. et al. Friction based welding technology for aluminium. **In:** 8th INTERNATIONAL CONFERENCE ON ALUMINIUM ALLOYS, 2002, Cambridge. Proceedings. Available in: http://www.twi.co.uk/content/spwmtjuly2002.html. Accessed in: September 25 2010.

[4] SCIALPI, A. et al. Mechanical analysis of ultra-thin friction stir welding joined sheets with dissimilar and similar materials, Materials & Design, v.29, n.5, p.928-936, 2008.

[5] KALLEE, S.W.; NICHOLAS, E.D.; THOMAS, W.M. Friction stir welding - invention, innovations and applications. **In:** INALCO 2001 - 8th INTERNATIONAL CONFERENCE ON JOINTS IN ALUMINIUM, 2001, Munich. Proceedings. Available in: http://www.twi.co.uk/content/spswkmar2001.html. Accessed in: September 25 2010.

[6] THOMAS, W.M.; JOHNSON, K.I.; WIESNER, C.S. Friction stir welding-recent developments in tool and process technologies, Advanced Engineering Materials, v.5, n.7, p.485-490, 2003.

[7] MISHRA, R.S.; MA, Z.Y. Friction stir welding and processing, Materials Science and Engineering R, v. 50, p.1-78, 2005.

[8] NANDAN, R.; DEBROY, T.; BHADESHIA, H.K.D.H. Recent advances in friction stir welding - Process, weldment, structure and properties, Progress in Materials Science, v.53, n.6, p.980-1023, 2008.

[9] BUFFA, G.; FRATINI, L.; SHIVPURI, R. Finite element studies on friction stir welding processes of tailored blanks, Computers & Structures, v.86, n.1-2, p.181-189, 2008.

[10] PEEL, M. et al. Microstructure, mechanical properties and residual stresses as a function of welding speed in aluminium AA5083 friction stir welds, Acta Materialia, v.51, n.16, p.4791-4801, 2003.

[11]TWI. Microstructure classification of friction stir welds. Available in: http://www.twi.co.uk/content/fswqual.html. Accessed in: September 25 2010.

[12] KALLEE, S.W. et al. Development and implementation of innovative joining processes in the automotive industry. **In:** DVS ANNUAL WELDING CONFERENCE 'GROßE SCHWEIßTECHNISCHE TAGUNG', 2005, Essen. Proceedings. Available in: http://www.twi.co.uk/content/spswksept2005.html. Accessed in: September 25 2010.

[13] KALLEE, S.W. Friction Stir Welding in Series Production. Automobil Produktion, 2004. Available in: http://www.twi.co.uk/content/spswkdec2004.html. Accessed in: September 25 2010.

[14] KALLEE, S.W. Friction stir welding - how to weld aluminium without melting it. **In:** Innovations for New Rail Business, 2001, London. Proceedings. Available in: http://www.twi.co.uk/content/spswkmay2001.html. Accessed in: September 25 2010.

[15] RODRIGUES, D.M. et al. Influence of FSW parameters on the microstructural and mechanical properties of AA 6016-T4 thin welds, Materials & Design, v.30, p.1913-1921, 2009.

[16] FULLER, C.B. et al. Evolution of microstructure and mechanical properties in naturally aged 7050 and 7075 Al friction stir welds, Materials Science and Engineering A, v.527, n.9, p.2233-2240, 2010.

[17] GENEVOIS, C. et al. Quantitative investigation of precipitation and mechanical behaviour for AA2024 friction stir welds, Acta Materialia, v.53, n.8, p.2447-2458, 2005.

[18] GENEVOIS, C.; DESCHAMPS, A.; VACHER, P. Comparative study on local and global mechanical properties of 2024 T351, 2024 T6 and 5251 O friction stir welds. Materials Science and Engineering A, v.415, n.1-2, p.162-170, 2006.

[19] SU, J.-Q. et al. Microstructural investigation of friction stir welded 7050-T651 Aluminum, Acta Materialia, v.51, p.713-729, 2003.

[20] SATO, Y.S.; PARK, S.H.C.; KOKAWA, H. Microstructural factors governing hardness in friction-stir welds of solid-solution-hardened Al alloys, Metallurgical and Materials Transactions A, v.32, n.12, p.3033-3042, 2001.

[21] LEE, W.B.; JUNG, S.B. The joint properties of copper by friction stir welding, Materials Letters, v.58, n.6, p.1041-1046, 2004.
[22] MERAN, C.; KOVAN, V. Microstructures and mechanical properties of friction stir welded dissimilar copper/brass joints, Materialwissenschaft Und Werkstofftechnik, v.39, n.8, p.521-530, 2008.
[23] XIE, G.M.; MA, Z.Y.; GENG, L. Development of a fine-grained microstructure and the properties of a nugget zone in friction stir welded pure copper, Scripta Materialia, v.57, n.2, p.73-76, 2007.
[24] PARK, H.S. et al. Microstructures and mechanical properties of friction stir welds of 60% Cu-40% Zn copper alloy, Materials Science and Engineering A, v.371, n.1-2, p.160- 169, 2004.
[25] MERAN, C. The joint properties of brass plates by friction stir welding, Materials & Design, v.27, n.9, p.719-726, 2006.
[26] ÇAM, G.; MISTIKOGLU, S.; PAKDIL, M. Microstructural and Mechanical Characterization of Friction Stir Butt Joint Welded 63% Cu-37% Zn Brass Plate, Welding Journal, v.88, n.11, p.225S-232S, 2009.
[27] LEITAO, C. et al. Formability of similar and dissimilar friction stir welded AA 5182-H111 and AA 6016-T4 tailored blanks, Materials & Design, vol. 30, n. 8, p. 3235-3242, 2009.
[28] LEITAO, C. et al. Mechanical behaviour of similar and dissimilar AA5182-H111 and AA6016-T4 thin friction stir welds, Materials & Design, v.30, n.1, p.101-108, 2009.
[29] LEAL, R.M. et al. Mechanical Behaviour of FSW Aluminium Tailored Blanks, Materials Science Forum, v.587-588, p.961-965, 2008.
[30] NANDAN, R. et al. Numerical modelling of 3D plastic flow and heat transfer during friction stir welding of stainless steel, Science and Technology of Welding and Joining, v.11, n.5, p.526-537, 2006.
[31] MURR, L.E. et al. Intercalation vortices and related microstructural features in the friction-stir welding of dissimilar metals, Materials Research Innovations, v.2, n.3, p.150-163, 1998.